PROCEEDINGS OF SPIE

SPIEDigitalLibrary.org/conference-proceedings-of-spie

MOSAIC optical relay module: optical design, performance, and flexure analysis

Ariadna Calcines, Marc Dubbeldam, Timothy Morris, Ewan Fitzsimons, Hermine Schnetler, et al.

Ariadna Calcines, Marc Dubbeldam, Timothy J. Morris, Ewan Fitzsimons, Hermine Schnetler, Mathieu Cohen, Jean-Philippe Amans, "MOSAIC optical relay module: optical design, performance, and flexure analysis," Proc. SPIE 10702, Ground-based and Airborne Instrumentation for Astronomy VII, 107029P (11 July 2018); doi: 10.1117/12.2313481

SPIE.

Event: SPIE Astronomical Telescopes + Instrumentation, 2018, Austin, Texas, United States

MOSAIC optical relay module: optical design, performance and flexure analysis

Ariadna Calcines*[a], Marc Dubbeldam[a], Timothy J. Morris[a], Ewan Fitzsimons[b], Hermine Schnetler[b], Mathieu Cohen[c], Jean-Philippe Amans[c]

[a]Durham University, Centre for Advanced Instrumentation, DH1 3LE, United Kingdom; [b]UK Technology Astronomy Centre, EH9 3HJ, United Kingdom; [c]Observatoire de Paris, 92195, Meudon, France.

ABSTRACT

The Optical Relay Module of the MOSAIC multiple-object spectrograph is used to relay 400-1800nm light picked off from the ELT focal plane to either a fibre-based integral field unit or a natural guide star wavefront sensor.
Here we present the preliminary optical design offering a telecentric exit beam with a focal-ratio of F/17.718 and the opto-mechanical analysis of flexures with a study of the impact in the optical layout performances such as: deviation of the PSF centroid, tip-tilt of the image focal plane, variations of the wavefront error, optical quality and pupil wandering at the deformable mirror position.

Keywords: MOSAIC, ELT, MOS spectrograph, optical design, flexure analysis.

1. INTRODUCTION

MOSAIC[1] (Figure 1) is the multi-object spectrograph of the Extremely Large Telescope[2] (ELT) covering a spectral range from 400 to 1800 nm, however, the desired wavelength interval is extended from 370 to 2500 nm. Its MOS capability[3] will provide unprecedented observations of objects ranging from stars at the very heart of the Milky Way to the most distant galaxies at the edge of the observable universe. The project is currently in Phase A and entering preliminary design phase starting in 2019.

The MOS capability is combined with Adaptive Optics[4]. Both, the Integral Field Unit (IFU) and natural guide star wavefront sensor, are illuminated using an Optical Relay Module (ORM), whose optical design is described in this paper.

2. OPTICAL RELAY MODULE

The Optical Relay Module (ORM) of the MOSAIC multi-object spectrograph is used to relay 400-1800nm light picked off from the ELT focal plane to either a fibre-based Integral Field Unit or a natural guide star wavefront sensor. MOSAIC contains 24 relay modules that are situated around the edge of the ELT focal plane (Figure 1). The relay modules must contain a means of path-length compensation to address different pickoff mirrors within the focal plane and, within ten of the 24 channels, also a deformable mirror to provide open-loop AO correction. These channels are mounted on the rotating MOSAIC structure and experience up to a 360 degree change in gravity vector during observations.

*ariadna.calcines@durham.ac.uk; phone +44 191 334 4814.

Ground-based and Airborne Instrumentation for Astronomy VII, edited by Christopher J. Evans, Luc Simard, Hideki Takami, Proc. of SPIE Vol. 10702, 107029P · © 2018 SPIE · CCC code: 0277-786X/18/$18 · doi: 10.1117/12.2313481

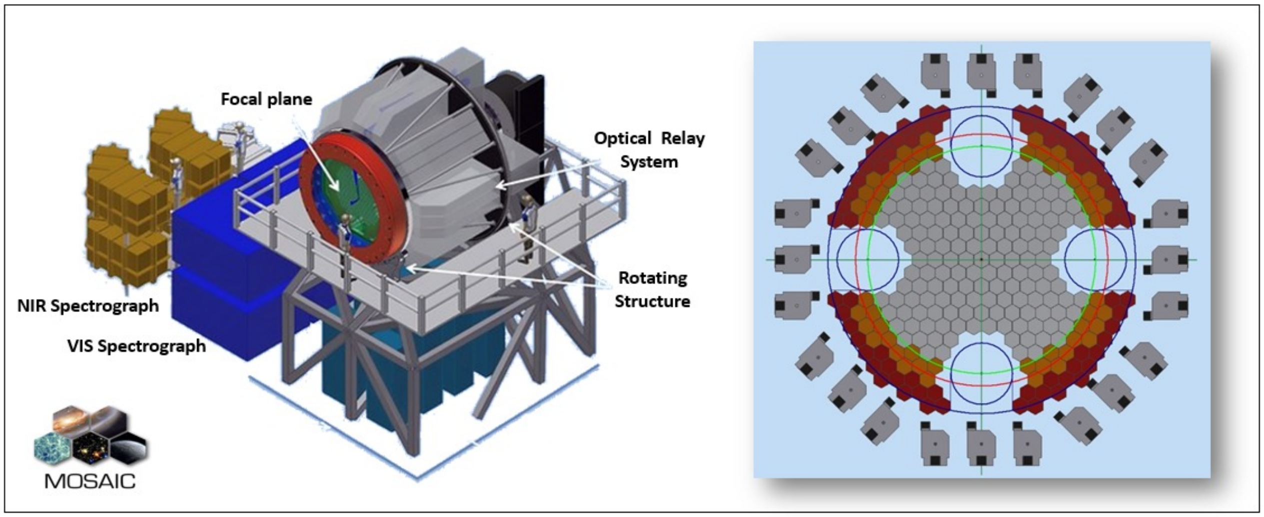

Figure 1: On the left, MOSAIC layout obtained from the ESO's website. On the right, twenty four beam steering mirrors arranged in an octagonal pattern around the ELT focal plane.

The MOSAIC Relay layout (Figure 2 and Figure 3) starts after light from the telescope image focal plane has been picked off using a flat mirror, Pick-Off Mirror (POM), to select the field of interest. This beam is then reflected towards a Beam Steering Mirror (BSM) at the ORM input. The BSM is also a flat mirror that can change orientation depending on the selected field to guarantee the same output direction for all fields towards the Trombone. The Trombone is a system composed of two translating flat mirrors (T1 & T2) to compensate the optical path differences. The Pupil Imaging Mirror (PIM) is an off-axis ellipsoid that generates a pupil image of 72 mm diameter on the deformable mirror (DM). Finally, the re-Imaging Mirror (IM) is an off-axis ellipsoid, which focuses the beam generating the output focus. A field lens makes the exit beam telecentric and the final focal-ratio is F/17.718. This paper presents an updated design of the ORM, now telecentric, with optimised optical quality and considering a larger pupil at the DM position of 72 mm diameter.

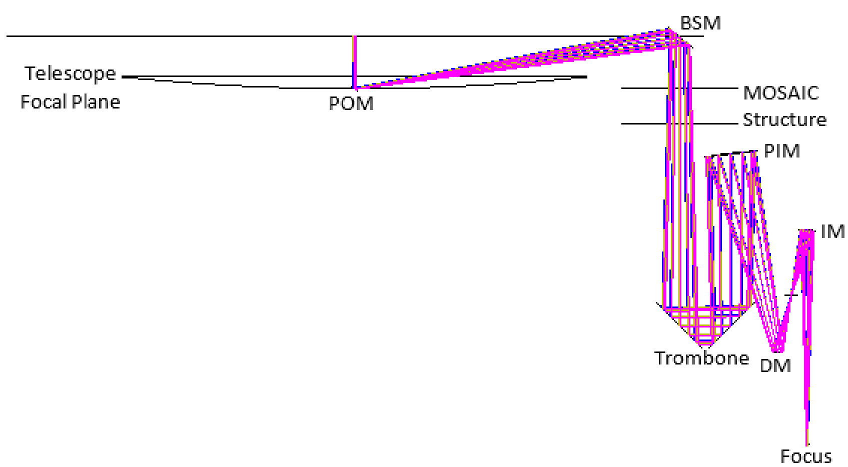

Figure 2. Layout of the Optical Relay Module.

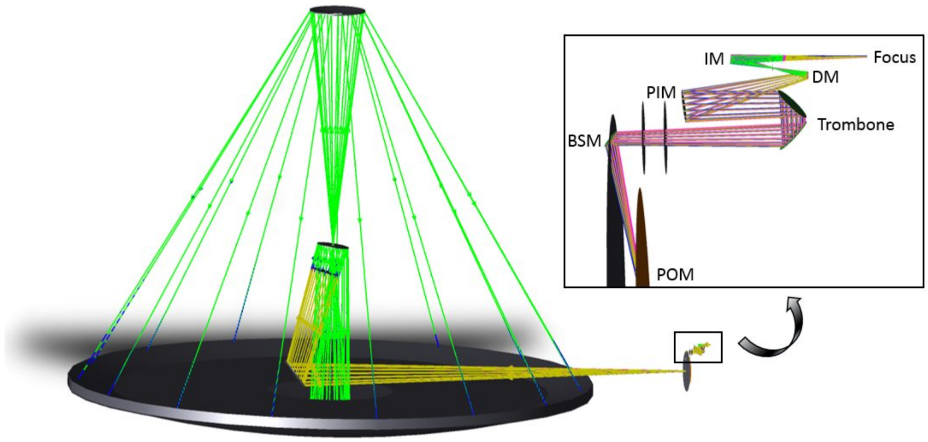

Figure 3. Location of the Optical Relay Module at the telescope.

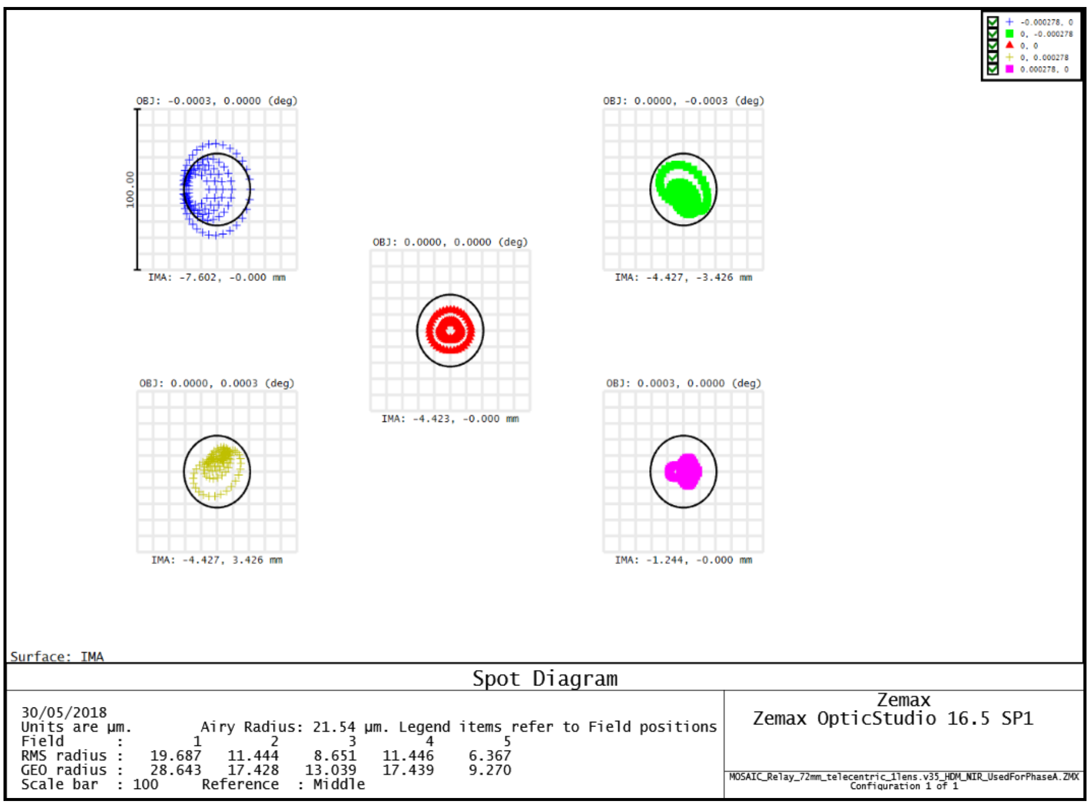

Figure 4: Optical quality obtained at the image focal plane for the nominal configuration at 1µm wavelength.

The deformable mirror uses up to 64 x 64 actuators for AO corrections. A small amount of the DM stroke (0.2143 µm as shown in Figure 5) is dedicated to aberration correction allowing diffraction-limited optical quality at 1µm wavelength, as shown in Figure 4.

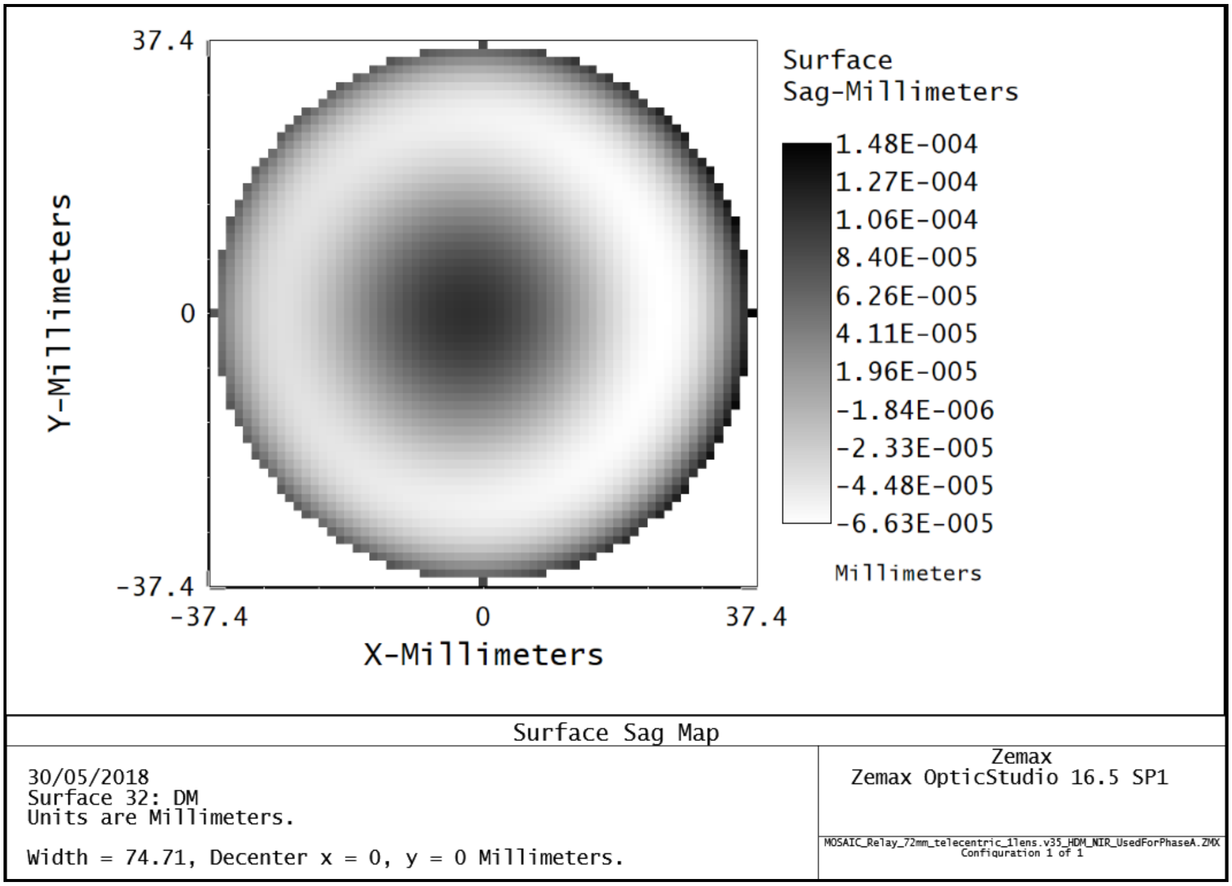

Figure 5: PTV stroke of 0.2143 µm required to improve the optical quality, which is now diffraction limited. The pupil size on the deformable mirror is 72 mm.

The RMS wavefront error is almost constant for all field points along the Y axis and under the diffraction limit as shown in Figure 6, where the blue curve represents the wavefront error across the field at 1 µm wavelength and the black curve on the top shows the diffraction limit. The average value evaluated at 1 µm wavelength is 48.90 nm RMS. It is, however, not constant along the X axis, where it varies from 48.00 nm and 98.50 nm.

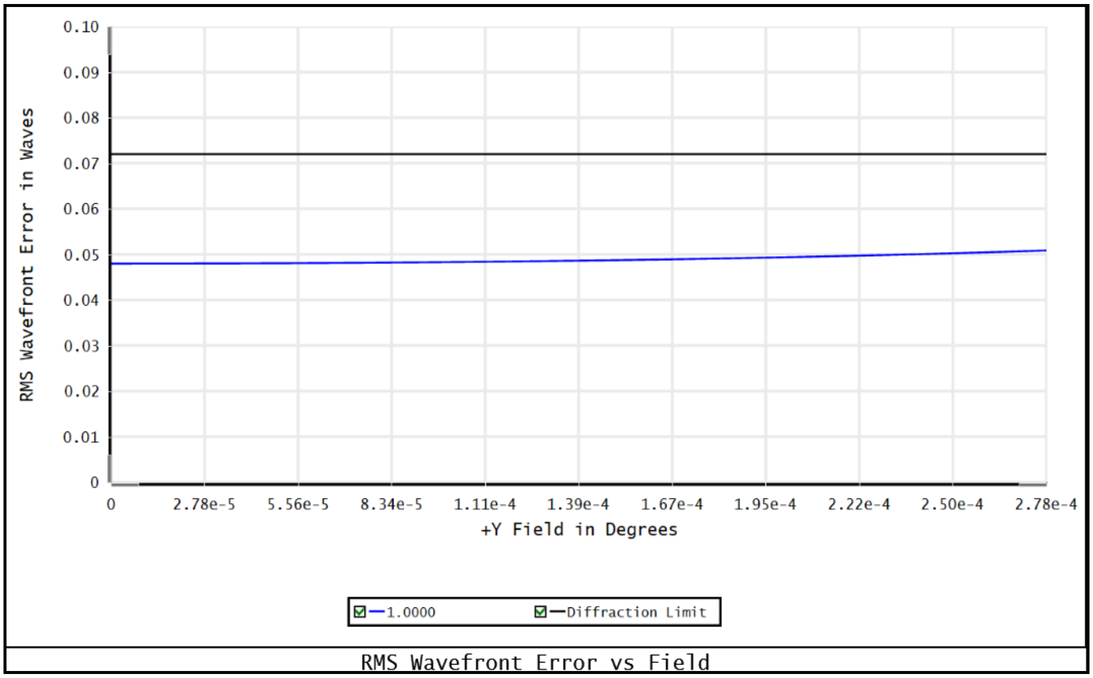

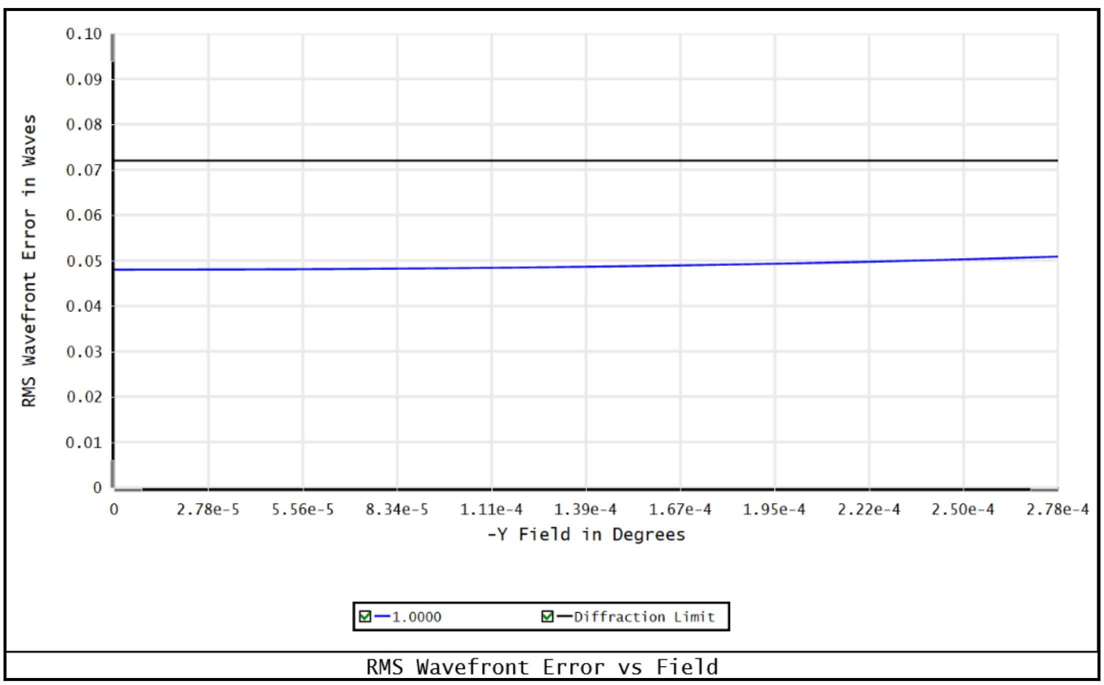

Figure 6: RMS wavefront error (blue) within the diffraction limit (black) for fields along the Y axis (+Y fields on the left, -Y fields on the right), evaluated at 1 μm wavelength.

3. SENSITIVITY ANALYSIS FOR PUPIL WANDERING

These analyses investigate the range of angles, Tilt X and Tilt Y, of the Pick-Off Mirror (POM) for a maximum pupil wandering of a $1/10^{th}$ of the sub-aperture at the deformable mirror (DM). The pupil wandering specification is then calculated as the diameter of the pupil a the DM (72 mm) divided by the number of sub-apertures (63) and divided by ten, which gives a maximum displacement of 0.114 mm.

The tolerance and sensitivity analysis were performed in Zemax defining a Merit Function to calculate the position of the chief ray at the deformable mirror and its variation with respect to the nominal case. No compensators were initially considered. Axes and degrees of freedom are defined in Figure 7.

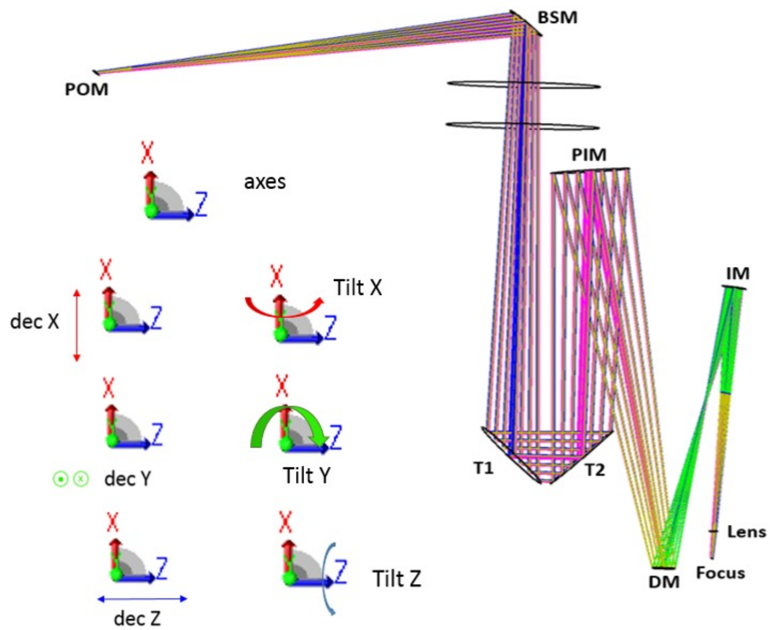

Figure 7: Definition of the axes and defined degrees of freedom in the Optical Relay Module design.

The sensitivity analysis and 100 Monte Carlo simulations were performed considering tolerances on Tilt X and Tilt Y on the POM of ± 0.080 milliradians. The analysis shows that a variation in the Tilt about the X axis has a bigger impact in the displacement of the pupil at the deformable mirror. A tilt of ±0.080 milliradians will move the pupil at the limit of the maximum pupil wandering specification along the X axis, while the same tilt about Y axis has a significantly smaller effect. This is due to the conic defined for the Pupil Imaging Mirror (PIM), which has an off-axis of 125 mm along the X axis and this establishes a preferential direction.

Based on the sensitivity analysis the maximum tolerances on Tilt X for the POM is ±0.080 milliradians, which also defines the accuracy required. Regarding the tolerances on Tilt Y for the POM and due to the low impact they have in the pupil wandering at the DM, these can be relaxed up to ±17.45 milliradians.

A hundred Monte Carlo simulations were performed for the tolerance analysis. In the first case considering a tolerance on Tilt X and Tilt Y of ±0.080 milliradians and in the second case for tolerances of ±0.080 milliradians on Tilt X and ±17.45 milliradians on Tilt Y. In both cases the departure of the chief ray was calculated, being 6.61% subaperture diameter or less in the first case for the 90% of the simulations and 8.56% subaperture diameter or less in the second case, in both cases within the specification of the pupil wandering (10%). Thus, the tolerances on Tilt X are ±0.080 milliradians and the tolerance on Tilt Y does not need high accuracy. If this degree of freedom needs to be implement, a tolerance of ±17.45 milliradians would meet the specifications.

A user script was defined in order to analyze the range of movement and accuracy required to compensate the pupil wandering at the DM position produced by the Tilt X and Tilt Y of the POM with Tilt X and Tilt Y of the BSM. A Tilt X of ±0.080 milliradians on the POM, which previously generated the maximum pupil wander allowed, now produces a negligible departure if it is compensated with the BSM.

As a result of the sensitivity analysis, the range of motion for the two degrees of freedom defined for the compensator (BSM) is obtained. A Tilt X= ± 0.00443°= ± 0.0773 milliradians and a Tilt Y=± 2.517°= ± 43.93 milliradians for the BSM would be required. These results are similar to those obtained from the Monte Carlo simulations, where the range of motion for Tilt X goes from -0.004127° to +0.004078°, this is from 0.072 to 0.071 milliradians and the interval for Tilt Y for the BSM is defined within the interval between -2.32 to 2.53 degrees, -40.49 milliradians to +44.16 milliradians.

The sensitivity and tolerance analysis were repeated for the BSM Tilt X and Tilt Y and without considering any compensator. Although initially the same tolerances as for the POM were considered for the BSM, the analysis revealed that a tolerance on Tilt X of ±0.0046° = ±0.080 milliradians would imply a pupil wandering of 10.31% subaperture diameter, which is larger than the specification. The sensitivity analysis also reveals that the system is much more sensitive to variation on tilt angles about the X axis than about the Y axis. In order to meet the specification the tolerances on Tilt X were reduced, up to ± 0.77 milliradians (±0.0044°). Tolerances on Tilt Y were kept as ±17.45 milliradians, however, due to the small impact on the pupil wandering these tolerances could be relaxed. Considering these tolerances the pupil wandering is kept within a 10% subaperture diameter, meeting the specification. The Monte Carlo simulations showed that for the 90% of the cases, the maximum departure of the chief ray at the DM position was 7.5% subaperture diameter.

4. FLEXURE ANALYSIS AND IMPACT IN THE OPTICAL PERFORMANCE

The impact of mechanical flexures in the optical performance of the ORM has been analyzed evaluating: variations in the pupil position at the deformable mirror, PSF centroid location at the relay image focal plane or variations of the RMS wavefront error.

The MOSAIC Relay Optical Module has 24 channels arranged in 8 sets of 3 channels. Each channel is subject to rotations. For each set the three channels (channel 1, channel 2, channel 3) will present different decentered distances and tilt angles due to their location with respect to the mounting points. Thus, the flexure analysis have been evaluated for three different configurations: 0 degrees, 30 degrees and 90 degrees rotation angle, where 0 degrees corresponds to the gravity vector (0, 0, -1) • g. The variations in decentered distances and tilt angles per channel for 0 degrees, 30 degrees and 90 degrees rotation angle are shown in Table 1, Table 2 and Table 3, respectively.

For the analysis, the position of the PSF centroid and the angle of inclination of the image focal plane were evaluated with the constraint of keeping the maximum pupil wandering at the deformable mirror position within a tenth of the subaperture diameter. A Merit function was defined to calculate the values associated to the nominal configuration (without flexures) and the departure when the flexures are included.

Table 1. Decentered distances and tilt angles for 0 degrees rotation angle obtained from the mechanical flexure analysis.

0 degrees rotation angle							
Component	**Channel**	**decX (mm)**	**decY (mm)**	**decZ (mm)**	**Tilt X (mrad)**	**Tilt Y (mrad)**	**Tilt Z (mrad)**
Trombone	1	0.000	0.000	-0.027	-0.010	0.012	0.001
	2	0.000	0.000	-0.029	0.000	0.012	0.001
	3	0.000	0.000	-0.028	0.010	0.011	0.001
PIM	1	0.001	0.000	-0.025	0.003	-0.003	-0.004
	2	0.001	0.000	-0.024	0.000	-0.008	0.000
	3	0.001	0.000	-0.025	-0.003	-0.006	0.003
DM	1	0.006	0.000	-0.027	-0.003	-0.006	0.002
	2	0.007	0.000	-0.027	0.000	-0.003	0.000
	3	0.007	0.000	-0.027	0.003	-0.003	-0.002
IM	1	0.006	0.000	-0.033	-0.001	0.007	0.000
	2	0.006	0.000	-0.033	0.000	0.007	0.000
	3	0.006	0.000	-0.033	0.002	0.007	0.000
Fibre Bundle	1	0.006	0.000	-0.027	-0.002	0.003	0.000
	2	0.007	0.000	-0.027	0.000	0.002	0.000
	3	0.006	0.000	-0.027	0.002	0.003	0.001

Table 2. Decentered distances and tilt angles for 30 degrees rotation angle obtained from the mechanical flexure analysis.

30 degrees rotation angle							
Component	**Channel**	**decX (mm)**	**decY (mm)**	**decZ (mm)**	**Tilt X (mrad)**	**Tilt Y (mrad)**	**Tilt Z (mrad)**
Trombone	1	0.000	0.003	-0.015	-0.036	0.011	0.001
	2	0.000	0.003	-0.025	-0.028	0.010	0.001
	3	0.000	0.003	-0.033	-0.019	0.010	0.001
PIM	1	0.000	0.016	-0.011	-0.032	-0.002	-0.005
	2	0.001	0.017	-0.021	-0.034	-0.006	-0.002
	3	0.001	0.017	-0.032	-0.036	-0.004	0.000
DM	1	0.005	0.024	-0.014	-0.032	-0.001	-0.001
	2	0.006	0.025	-0.024	-0.030	0.000	-0.003
	3	0.007	0.025	-0.033	-0.027	-0.004	-0.004
IM	1	0.005	0.032	-0.019	-0.032	0.006	0.000
	2	0.005	0.032	-0.029	-0.031	0.006	0.000
	3	0.005	0.032	-0.038	-0.030	0.006	0.000
Fibre Bundle	1	0.006	0.031	-0.014	-0.032	0.003	0.000
	2	0.006	0.031	-0.024	-0.030	0.002	0.000
	3	0.006	0.030	-0.033	-0.028	0.002	0.000

Table 3. Decentered distances and tilt angles for 90 degrees rotation angle obtained from the mechanical flexure analysis.

90 degrees rotation angle							
Component	**Channel**	**decX (mm)**	**decY (mm)**	**decZ (mm)**	**Tilt X (mrad)**	**Tilt Y (mrad)**	**Tilt Z (mrad)**
Trombone	1	0.000	0.006	0.017	-0.054	0.000	0.000
	2	0.000	0.006	0.000	-0.057	0.000	0.001
	3	0.000	0.005	-0.017	-0.055	0.000	0.001
PIM	1	-0.001	0.033	0.021	-0.068	0.002	-0.004
	2	0.000	0.033	0.000	-0.068	0.002	-0.004
	3	0.002	0.033	-0.021	-0.068	0.003	-0.004
DM	1	0.000	0.049	0.018	-0.060	0.009	-0.004
	2	0.000	0.049	0.000	-0.060	0.004	-0.005
	3	0.001	0.049	-0.018	-0.059	-0.003	-0.004
IM	1	-0.001	0.063	0.019	-0.062	0.001	0.000
	2	0.000	0.063	0.000	-0.062	0.000	0.000
	3	0.001	0.063	-0.020	-0.062	0.000	0.000
Fibre Bundle	1	0.000	0.061	0.018	-0.060	0.000	0.000
	2	0.000	0.061	0.000	-0.060	0.000	0.000
	3	0.000	0.061	-0.019	-0.060	0.000	0.000

A comparison of the flexure effects for the three configurations and three channels is presented in Table 4, where the first column on the left indicates the configuration (0 deg, 30 deg or 90 deg) and the channel number (1, 2, 3); the second column shows the pupil motion at the deformable mirror; the third column presents the PSF centroid departure at the image focal plane in local coordinates; the fourth column shows the variation of the exit angle and the fifth column presents the change in RMS wavefront error. All changes have been measured with respect to the nominal values. No significant changes on optical quality were found in the analysis. For each configuration the maximum deviation of the PSF centroid corresponds to channel 2. In these cases, this effect can be compensated which can be compensated by tilting the Beam Steering Mirror about the X axis -8.859E-04 degrees for channel 1, -4.93E-03 degrees for channel 2 and -8.546E-03 degrees for channel 3.

Table 4. Deviations produced by the effect of the flexures on each channel and configuration. The maximum deviation of the PSF centroid with respect to the nominal case corresponds to channel 2 for the three configurations. The percentage in the second column indicates the pupil motion in terms of sub-aperture diameter and it is only indicated in the cases that the specification is exceeded. This can be compensated with the Beam Steering Mirror (BSM). The pupil diameter at the deformable mirror is 72 mm. The maximum allowed pupil motion is 10% of the sub-aperture diameter, equivalent to 0.114 mm.

Config., Channel	**Pupil motion at DM**	**PSF centroid**	**Variation exit angle**	**Change RMS WFE**
1,1	Δx= -0.041 mm Δy= 8.851E-03 mm	Δx= -0.041 mm Δy= -0.039 mm Δz= 0 mm	1.601E-03 deg	36.00 nm (centroid) 34.39 nm (chief ray)
1,2	Δx= -3.733E-04 mm Δy= -8.851E-03 mm	Δx= -0.070 mm Δy= 0.040 mm Δz= 0 mm	1.821E-03 deg	36.00 nm (centroid) 34.39 nm (chief ray)
1,3	Δx= -3.676E-04 mm Δy=1.717E-08 mm	Δx= -0.088 mm Δy= -4.029E-08 mm Δz= 0 mm	1.956E-03 deg	36.00 nm (centroid) 34.39 nm (chief ray)
2,1	Δx= -5.039E-04 mm Δy= -0.231 mm (20.26%)	Δx= 5.923E-03 mm Δy= 0.386 mm Δz= 0 mm	-6.434E-04 deg	26.85 nm (centroid) 28.90 nm (chief ray)
2,2	Δx=-4.237E-04 mm Δy= -0.231 mm (20.265%)	Δx= 0.021 mm Δy=0.389 mm Δz= 0 mm	-1.038E-04 deg	28.84 nm (centroid) 28.90 nm (chief ray)
2,3	Δx= -4.614E-04 mm Δy= -0.231 mm (20.26%)	Δx=5.896E-03 mm Δy=0.386 mm Δz= 0 mm	-3.379E-04 deg	14.00 nm (centroid) 18.11 nm (chief ray)
3,1	Δx= -4.164E-04 mm Δy= -0.109 mm	Δx= -0.036 mm Δy= 0.163 mm Δz= 0 mm	1.173E-03 deg	20.00 nm (centroid) 18.11 nm (chief ray)
3,2	Δx= -3.641E-04 mm Δy= -0.122 mm (10.67%)	Δx= -0.054 mm Δy= 0.224 mm Δz= 0 mm	1.507E-03 deg	43.83 nm (centroid) 43.62 nm (chief ray)
3,3	Δx= -3.78E-04 mm Δ-0.116 mm (10.175%)	Δx= -0.075 mm Δy= 0.194 mm Δz= 0 mm	1.562E-03 deg	32.56 nm (centroid) 31.75 nm (chief ray)

5. CONCLUSIONS

The MOSAIC Optical Relay Module (ORM) is used to relay 400-1800nm light picked off from the ELT focal plane to either a fibre-based Integral Field Unit or a natural guide star wavefront sensor. The optical layout has been modified to offer an output telecentric beam with a focal-ratio of F/17.718 with a diffraction limited optical quality and using a 72 mm diameter pupil at the deformable mirror.

MOSAIC contains 24 relay modules that are situated around the edge of the ELT focal plane. The relay modules include mechanical degrees of freedom for the optics and to allow optical path length compensation. And, although the optical design meets specifications, the mechanical flexures produce modifications in the ORM optical performance. They increase the RMS wavefront error; produce a pupil motion at the deformable mirror position in some cases larger than the 10% of the sub-aperture diameter allowed; they change the PSF centroid position at the image focal plane and the output angle. All these effects have been analyzed for three channels at three configurations: 0 degrees, 30 degrees and 90 degrees rotation. The maximum departure of the PSF centroid at the image focal plane was obtained for channel 2 in all cases, which can be compensated by tilting the Beam Steering Mirror about the X axis -8.859E-04 degrees for channel 1, -4.93E-03 degrees for channel 2 and -8.546E-03 degrees for channel 3.

Sensitivity and tolerances analysis were also performed, in particular on the Pick-Off Mirror (POM) to guarantee a maximum pupil wandering at the deformable mirror position of a tenth of the sub-aperture of the deformable mirror, which is 0.114 mm.

The analysis showed a preferential direction, where the chief ray position was not as sensitive to tilt angles about the Y axis for the POM as to tilt angles about the X axis. This is due to the Pupil Imaging Mirror, which is decentered along the X direction. As a consequence, the range of tilt angles allowed for the POM to meet the pupil wandering specification is ±0.080 milliradians for Tilt X and ±17.45 milliradians for Tilt Y. The departure due to these tilt angles can be compensated with tip and tilt of the BSM, requiring a range of motion of Tilt X defined within the interval between -0.072 milliradians and +0.071 milliradians, and an interval of Tilt Y angles within [-40.491, +44.234] milliradians.

The sensitivity and tolerances analysis were also performed for the Beam Steering Mirror (BSM) without defining any extra compensator, and, as in the previous case, a maximum pupil wandering of 10% sub-aperture diameter at the DM position was defined as the constraint. The pupil location was much more sensitive to changes on Tilt X of the BSM than changes on Tilt Y. Tolerances on Tilt X need to be reduced up to ± 0.77 milliradians in order to meet the specifications.

REFERENCES

[1] Hammer, F.; Morris, S.; Kaper, L.; Barbury, B.; Cuby, J. G.; Roth, M.; Jagourel, P.; Evans, C. J.; Puech, M.; Fitzsimons, E.; Dalton, G.; Rodrigues, M., "The E-ELT multi-object spectrograph: latest news from MOSAIC", Proc. SPIE 9908, 990824 (2016).

[2] McPherson, A.; Spyromilio, J.; Kissler-Patig, M.; Ramsay, S.; Brunetto, E.; Dierickx, P.; Cassali, M., "E-ELT update of project and effect of change to 39m design", Proc. SPIE 8444, 84441F (2012).

[3] Evans, C. J.; Puech, M.; Rodrigues, M.; Barbury, B.; Cuby, J.-G.; Dalton, G.; Fitzsimons, E.; Hammer, F.; Jagourel, P.; Kaper, L.; Morris, S. L.; Morris, T.J., "Science requirements and trade-offs for the MOSAIC instrument for the European ELT", Proc. SPIE 9908, 99089j(2016).

[4] Morris, T.; Basden, A.; Buey, T.; Chemla, F.; Conan, J.-M.; Fitzsimons, E.; Fusco, T.; Gendron, E.; Hammer, F.; Jagourel, P.; Morel, C.; Myers, R.; Neichel, B.; Petit, C.; Rodrigues, M.; Rousset, G., "Adaptive optics for MOSAIC: design and performance of the wide(st)-field AO system for the E-ELT", Proc. SPIE 9909, 99091I (2016).